AD-A170 560 MICROMECHANICS II(U) HARVARD UNIV CAMBRIDGE MA DIV OF APPLIED SCIENCES B BUDIANSKY JUN 86 MECH-82 N00014-84-K-0510 1/1

UNCLASSIFIED F/G 20/11 NL

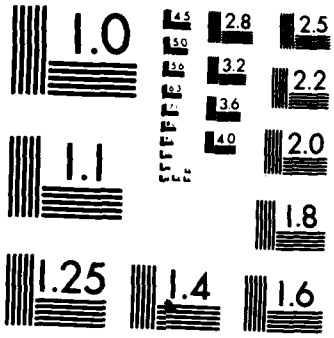

MICROCOPY RESOLUTION TEST CHART
NATIONAL BUREAU OF STANDARDS-1963-A

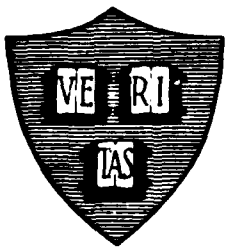

MECH-82

MICROMECHANICS II

Bernard Budiansky

Contract N00014-84-K-0510

Division of Applied Sciences
HARVARD UNIVERSITY
Cambridge, Massachusetts 02138

June 1986

Presented at Tenth U. S. National Congress of Applied Mechanics, The University of Texas, Austin, Texas, June 16-20, 1986

MICROMECHANICS II

BERNARD BUDIANSKY

Division of Applied Sciences
Harvard University
Cambridge, Massachusetts 02138

ABSTRACT

Several current studies in the micromechanics of solid bodies are reviewed. As in many such investigations, methods of continuum and structural mechanics are used in the analysis of models at microscopic levels with the aim of increasing understanding of material behavior in the large. The works described herein are concerned with the fracture resistance of toughened ceramics, the interfacial stress analysis of hard particles in ductile metals, and the elastic behavior of lungs.

INTRODUCTION

Micromechanics is the currently fashionable designation of what is really an old subject, but one that is receiving increasing attention from theoreticians in applied mechanics. Armed with their repertoire of analytical tools, they try to relate the overall deformation and strength properties of materials to the behaviors and interactions of their microscopic constituents. Typically, such constituents are grains, particles, fibers, with sizes of the order of microns to millimeters. An earlier survey by the writer, in the spirit of the present one, was given in [1]; a new set of topics is discussed here.

CERAMICS

Because they stay solid and hard at elevated temperatures, ceramics appear to hold considerable potential for use in engines, where the payoff in thermodynamic efficiency increases with operating temperature. The trouble with ceramics, however, is that at moderate temperatures they are fragile, and fracture easily. Considerable effort is therefore currently devoted to a search for ways to toughen ceramics by various techniques, usually involving reinforcement by the addition of strengthening constituents. *Transformation toughening* -- in which unstable particles undergo phase-transformation expansions in the vicinity of growing cracks, and hence act as self-sealing agents [1, 2, 3] -- has been receiving continued attention (e.g. [4], [5]). Aspects of the fracture of *fiber-reinforced ceramics* were recently studied in [6]. Here, we turn first to some current theoretical research on the fracture of *cermets* -- ceramics reinforced by strong metallic particles.

Particulate Toughening

The essential physical process that seems to be involved in *particulate toughening* (e.g. [7,8]) is that of *crack-bridging*. If a crack in the ceramic matrix tries to extend by going through the metallic inclusions, instead of bypassing them; and if the bonds between the particles and the ceramic are strong; and if the particle itself is strong (three big ifs!); then cracks in the ceramic that have grown to some extent will be bridged by intact particles (Fig. 1), and continued crack growth will thereby be inhibited. A detailed discussion of the conditions under which bridging may be encouraged will not be given here; suffice it to say that cracks tend to be attracted to particles when the particle stiffness is lower than that of the matrix material, but [8] initial thermal stress may also play an important role. Attention will be directed here to the theoretical estimation of the magnitude of the toughness enhancement to be expected if bridging does indeed occur.

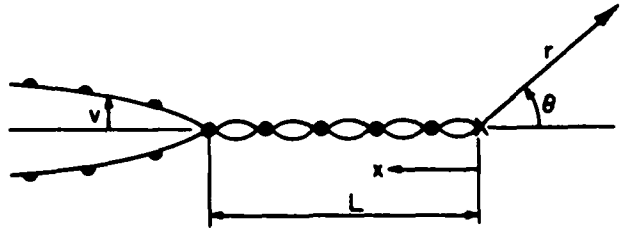

Fig. 1 Partially bridged crack

We contemplate the following *small-scale bridging* situation (Fig. 1): An "applied" stress-intensity factor K produces the standard crack tip stresses

$$\sigma_{\alpha\beta} = \left(\frac{K}{\sqrt{2\pi r}}\right) f_{\alpha\beta}(\theta) \qquad (1)$$

but these are reduced by the effects of the bridges that keep the crack faces closed, at discrete intervals, up to a length L. The phrase "small-scale" means that the bridge-length L is small relative to the crack length, the specimen size, and distances from the crack to the specimen boundaries. Under these conditions, the stresses (1) constitute a *far-field* distribution relative to the crack tip.

Now we want the picture in Fig. 1 to represent steady-state crack growth to the right, with both L and K remaining unchanged. Two strength conditions will accordingly be imposed: matrix stresses very near the crack tip (appropriately averaged with respect to thickness normal to the plane of Fig. 1) should be given by Eq. (1), with K replaced by K_m, the toughness of the ceramic; and the stress on the "last" intact particle, at x = L, will be set equal to S, the particle breaking strength. We want to calculate K, which is now the toughness of the reinforced material, in terms of K_m, S, the volume concentration c of particles, and the particle radius a.

Dimensional analysis suggests a relation of the form

$$K/K_m = F\left(\frac{S\sqrt{a}}{K_m}, c\right) \qquad (2)$$

and this immediately indicates a perhaps unexpected conclusion: for S and c fixed, toughness should increase with particle size. A recent thesis by Sigl [9] indicates that such effects have indeed been observed. (But note that S might well be a decreasing function of particle size.)

In a current study [10], the following integral equation has been written for the particle stress distribution $\sigma_p(x)$ (interpreted as the stress averaged over all particles at x):

$$\beta[\pi\,\bar{a}\,(1-\nu^2)/(2E)]\,\sigma_p(x) = 4(1-\nu^2)K\sqrt{x}/(E\sqrt{2\pi}) - 4(1-\nu^2)/(\pi E)\int_0^L \log[(\sqrt{x}+\sqrt{t})/(|x-t|)^{1/2}\,c\sigma_p(t)dt \qquad (3)$$

Here the first term on the right is what the crack-face displacement v(x) would be in the absence of bridging; the term containing the integral represents the closing effect of the bridging-particle stresses; and the left-hand side is an independent estimate of the net crack-face displacement in the bridged zone, again averaged through the thickness. Without the factor β, this term is the average surface displacement of a half-space subjected to stress $\sigma_p(x)$ on a disk of radius $\bar{a} = \sqrt{2/3}a$, the root-mean-square radius of disks intercepted by a plane through a random field of spherical particles of radius a. The factor β corrects this displacement for the simultaneous presence of many particles tying down the surface, and has been approximated in [10] by

$$\beta = (1-c)(1-\sqrt{c}) \qquad (4)$$

(The Young's modulus E and Poisson's ratio ν in (3) should refer to those of the composite material, but we will assume that they are the same as those of the ceramic; anyhow, they factor out here.)

In terms of the solution of the integral equation (3) for $\sigma_p(x)$, the aforementiond steady-state cracking conditions will be written as

$$\sigma_p(L) = S \qquad (5)$$

and

$$K = \sqrt{\frac{2}{\pi}}\int_0^L \frac{c\sigma_p(x)dx}{\sqrt{2}} = K_m(1-c)^{1/2} \qquad (6)$$

Equation (5) stipulates the breaking of the "last" particle, and Eq. (6) asserts that the r.m.s. value of the stress-intensity factor in the ceramic along its presumed straight, but interrupted crack front, attains the critical value K_m.

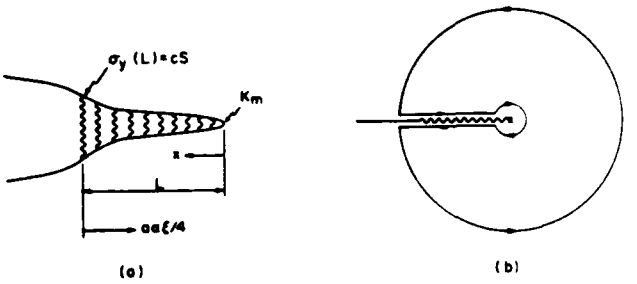

Fig. 2 (a) Spring model, (b) J-integral path

Equations (5-6) can now be regarded as parametric equations relating K, K_m, and S, via assumed values of L, and the solution of (3) for $\sigma_p(x)$. (Of course, the formulation can be conveniently non-dimensionalized.) But, remarkably, the desired final result, namely the function F in Eq. (2), can be found without solving the integral equation, because Rice's ubiquitous J-integral can be exploited. To do so, it is useful to think of (3) as an equation governing the distributed stress

$$\sigma_y(x) = c\sigma_p(x) \qquad (7)$$

in a line of springs (Fig. 2a) joining the crack faces. The non-dimensional compliance α in the stretch-stress relation

$$2v \equiv \delta = \alpha\,[\sigma_y\, a(1-\nu^2)/E] \qquad (8)$$

would then be given by

$$\alpha = \beta\pi\sqrt{2/3}\,/c \qquad (9)$$

Writing the J-integral for the path in Fig. 2b gives

$$K^2(1-\nu^2)/E = K_m^2(1-c)(1-\nu^2)/E + \tfrac{1}{2}\alpha\,\sigma_y^2(L)a(1-\nu^2)/E \qquad (10)$$

where the (1–c) term, as in (6), reflects the fact that only the matrix is cracked along the crack edge. Using (4), (5), (7), (9) in (10) gives

$$(K/K_m)/(1-c)^{1/2} = \{1 + (\pi/\sqrt{6})S^2[ac(1-\sqrt{c})]/K_m^2\}^{1/2} \qquad (11)$$

as the desired equation for particulate toughening, plotted in Fig. 3.

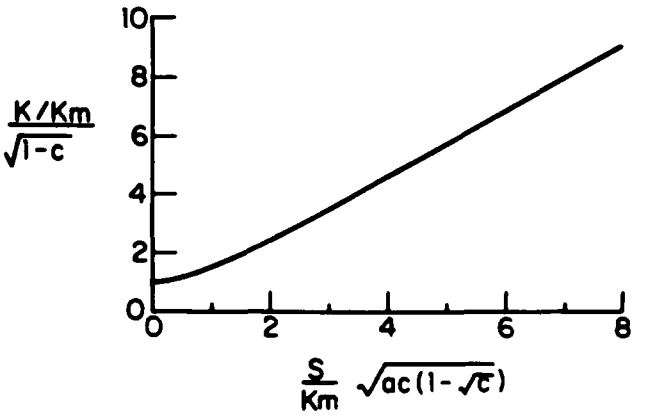

Fig. 3 Particulate toughening

There is at present a serious obstacle to applying (11) to real

systems, namely ignorance concerning the particle strength S. Because of the way it is constrained by the elastic ceramic, stresses in a bridging particle will tend to be nearly hydrostatic, with plastic flow greatly inhibited. On the other hand, each bridging particle is subjected locally to intense stresses where it is hit by the crack in the ceramic. Some recent estimates [12], based on ideal plasticity suggest that $S > 6\sigma_Y$, where σ_Y is the uniaxial yield stress, might be anticipated. Working backwards from Eq. (11) with a few experimental toughness measurements on several reinforced ceramics points to inferred values of S about ten times the uniaxial strength of the particle material. The problem of calculating the strength of a ductile bridging particle is open.

It should be noted that the magnitude of the effective compliance α in Eq. (8) may really be higher than we have assumed, with the consequence that values of S inferred from Eq. (11) for a given toughening would not be quite so big. Perhaps some interface sliding occurs near the equator of each bridging particle before it fails, increasing the average crack opening displacement. Such sliding would, in addition, reduce the constraint on the particle, letting it deform plastically more. In fact, the effective stretch-stress relation in our spring model would then no longer be linear. More of this when we look at bridging *fibers* later.

A partial check of the theory that does not involve S can be made by solving (3) for a given bridge length L, and then using (6) to see how K, K_m, and L are related. (Alternatively, we could substitute the calculated value of $\sigma_p(L)$ for S in Eq. (11), thereby finding K/K_m for the assumed value of L.) An approximate solution of (3) provided the non-dimensional results shown in Fig. 4, which also shows two available experimental points. The agreement is encouraging.

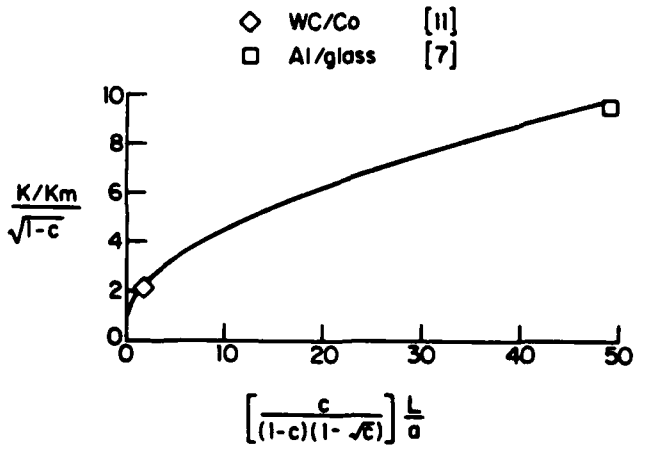

Fig. 4 Toughening vs. bridge length

Besides showing how toughening is related to bridge length, Fig. 4 can be interpreted as a *resistance curve*, relating applied K to crack extension. An initially unbridged crack will grow into the matrix under increasing K until the bridge length L, equal to the crack extension, is such that the relationships in Figs. 3 and 4 are both met at the same K. Subsequently, K and L remain constant as steady-state cracking proceeds.

The numerical solution of (3) needs some care, especially for large values of L/a, because then the distribution of $\sigma_p(x)$ peaks sharply at $x = L$. Fortunately, an exact solution is available for $L \to \infty$, which can be used to guide the numerics for finite L. With

$$(L-x)/a = \alpha\xi/4 \tag{12}$$

and

$$\sigma_y\sqrt{a}/K = 2g(\xi)/\sqrt{\alpha} \tag{13}$$

we find from (3), for $L \to \infty$,

$$g'(\xi) - \frac{1}{\pi}\int_0^\infty \frac{g(\eta)d\eta}{\xi-\eta} = 0 \tag{14}$$

and the far-field conditions require $g \sim 1/\sqrt{2\pi\xi}$ for $\xi \to \infty$. This is a setup for a Wiener-Hopf solution, which gives

$$g(\xi) \sim 1/\sqrt{2} - \xi[1 - \gamma - \log\xi]/(\pi\sqrt{2}) \tag{15}$$

$$(\gamma = .5722...)$$

for $\xi \to \infty$, and

$$g(\xi) \sim 1/\sqrt{2\pi\xi} - [\psi(\tfrac{3}{2}) - 1 - \log\xi]/(2\pi\xi)^{3/2} + \ldots \tag{16}$$

$$(\psi(z) \equiv \Gamma'(z)/\Gamma(z))$$

for $\xi \to \infty$. Note that since the "last" spring is now at $\xi = 0$, and since $L \to \infty$ implies $K_m \to 0$, the analytical result $g(0) = 1/\sqrt{2}$ is consistent with the J-integral relation (10).

Synergism: Combined Bridging and Transformation Toughening

The analysis in [2] of small-scale transformation toughening provided the energy-based result

$$K^2(1-\nu^2)/E = K_m^2(1-\nu^2)/E + \xi_T \tag{17}$$

for the enhanced stiffness K, where ξ_T is a residual wake energy-per-unit-length produced by phase-transforming particles. A fair approximation to ξ_T (for so-called "super-critical" transformations) was given by

$$\xi_T = \left[\frac{\sqrt{3}(1+\nu)^2}{6\pi}\right](K^2/\sigma_m^c)c_T\theta_p^T \tag{18}$$

where θ_p^T is the volumetric strain of a freely transforming particle, c_T is the volume concentration of transforming particles, and σ_m^c is the critical mean stress for the occurrence of phase transformation. The result for transformation toughening is then (approximately)

$$K/K_m = \left\{1 - \left[\frac{\sqrt{3}}{6\pi}\left(\frac{1+\nu}{1-\nu}\right)\right]\frac{Ec_T\theta^T}{\sigma_m^c}\right\}^{-1/2} \tag{19}$$

It now appears [5] that the theory of [2] has to be developed further to include additional effects, notably the influence of shear stresses on triggering the phase transformations. Nevertheless, it is instructive to exploit Eq. (17) to see how the effects of phase transforming and bridging particles might interact. Equation (10), derived from a J-integral, can also be regarded as an energy-balance relation, and so if we write a combined energy equation, presuming that (18) still provides a reasonable approximation for ξ_T, we get

$$K^2(1-\nu^2)/E = K_m^2(1-c)(1-\nu^2)/E + \tfrac{1}{2}\alpha S^2c^2a(1-\nu^2)/E$$

$$+ \left[\frac{\sqrt{3}(1+\nu)^2}{6\pi}\right][K^2c_T\theta^T/\sigma_m^c] \tag{20}$$

where we used $\sigma_y(L) = cS$. Then the result for the combined toughening is described by the *product* of (11) and (19):

$$\frac{(K/K_m)}{(1-c)^{1/2}} = \left\{ \frac{1 + \frac{\pi}{\sqrt{6}} \frac{S^2}{K_m^2} [ac(1-\sqrt{c})]}{1 - \frac{\sqrt{3}}{6\pi} \left(\frac{1+\nu}{1-\nu}\right) \left(\frac{Ec_T\theta^T}{\sigma_m^c}\right)} \right\}^{1/2} \qquad (21)$$

The implication is that $\Delta K \equiv K - K_m$ is larger than the sum of the ΔK's that would be produced separately by each of the toughening agents.

Bridging Fibers

The work in [6] was concerned with steady-state matrix cracking in a ceramic reinforced by long aligned fibers that remain unbroken. If the fibers, of radius a, are held in the matrix by friction, long cracks normal to the fibers were found to propagate at the critical stress σ_{cr} given in Fig. 5 in terms of reference stresses σ_0 and σ_1 defined by

$$\frac{\sigma_0}{E} = B(c) \left[\frac{6c^2 E_f}{(1-c)^2 E(1+\nu_m)} \right]^{1/4} \left[\frac{K_m^2 (1-\nu_m^2)}{E_m^2 a} \right]^{1/2} \qquad (22)$$

$$\frac{\sigma_1}{E} = \left[\frac{6c^2 E_f \tau}{(1-c) E E_m} \right]^{1/3} \left[\frac{K_m^2 (1-\nu_m^2)}{E_m^2 a} \right]^{1/3} \qquad (23)$$

Here τ is the sliding shear resistance of the fiber-matrix inferface; E_f, E_m, and $E = cE_f + (1-c)E_m$ are the longitudinal moduli of the fiber,

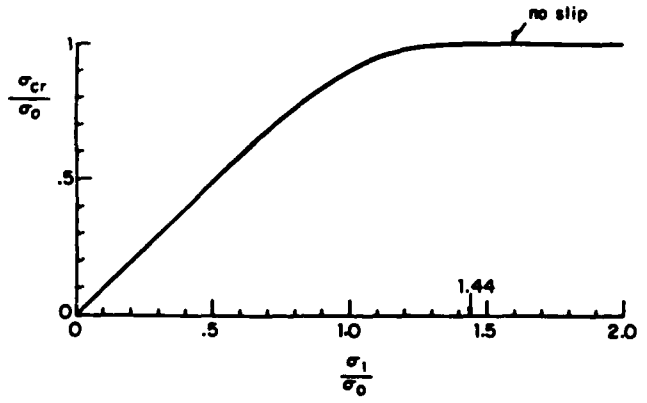

Fig. 5 Matrix cracking stress

matrix, and composite, respectively; and B(c) is a utility constant defined by

$$B = \left[\frac{2(1-c)^3}{-6\log c - 3(1-c)(3-c)} \right]^{1/4} \qquad (24)$$

Fiber-matrix interface slip will not occur during matrix cracking if $\sigma_1/\sigma_0 > 3^{1/3}$, in which case $\sigma_{cr} = \sigma_0$. Otherwise, sliding will take place, and $\sigma_{cr} = \sigma_1$ becomes a good approximation.

But now let us consider, as in [12, 13], the toughness of a ceramic when a crack cuts through fibers, and then a picture like that in Fig. 1 applies, with intact fibers normal to the crack replacing particles along the bridged portion. Once again, a J-integral can be written (Fig. 2), this time as

$$K^2(1-\nu^2)/(AE) = K_m^2(1-c)(1-\nu^2)/E_m + V(cS) \qquad (25)$$

where A is a constant that takes into account the anisotropy of the composite material; S is the fiber strength; and $V(\sigma_y)$ is the strain-energy function of the stress σ_y in distributed springs that appropriately model the bridging fibers. To find out what V should be, we can simply retrace the derivation of Fig. 5, using a similar spring model in the formulation of the matrix-cracking problem in the case of unbroken fibers. The outcome is

$$V(\sigma_y) = \left[\frac{K_m^2 (1-c)(1-\nu_m^2)}{E_m} \right] P(\sigma_y) . \qquad (26)$$

where

$$P(\sigma_y) = (\sigma_y/\sigma_0)^2 \qquad (27)$$

$$\text{for} \quad (\sigma_y/\sigma_0) \le (\sigma_1/\sigma_0)^3/3$$

$$= (\sigma_y/\sigma_1)^3 + (\sigma_y/\sigma_1)(\sigma/\sigma_1)^4/3 - (\sigma_1/\sigma_0)^6/27 \qquad (28)$$

$$\text{for} \quad (\sigma_y/\sigma_0) \ge (\sigma_1/\sigma_0)^3/3$$

Then the result for toughening becomes

$$\frac{(K/K_m)}{[AE(1-c)/E_m)]^{1/2}} = [1 + P(cS)]^{1/2} \qquad (29)$$

Note that for small S, P is quadratic, as in Eq. (12) for particle bridging; but for S large, $P = O(S^3)$, and the toughness becomes proportional to $S^{3/2}$. Note that the effect of decreasing the sliding resistance τ is to decrease σ_1, and hence to *increase* the toughness; but eventually, for small enough τ, the bridging length needed to attain the enhanced toughness would become inordinately large, involving unacceptably long matrix cracks. The question of an optimum choice for τ has received some preliminary study in [13], but needs further exploration.

METALS

Some basic calculations have recently been made by Wilner [14] concerning interface stresses at hard, second-phase particles in ductile metals. It is now commonplace that metals often fracture by the process of void nucleation, growth, and coalescence, and it is to the first of these that Wilner's work is relevant. Void nucleation at inclusions tends to occur by interfacial separation when the particles are sphere-like (whereas elongated particles often fracture first). The analysis of [14] contemplates an isolated, spherical, elastic inclusion in an infinite elastic-plastic matrix subjected to a monotonically increasing axisymmetric stress-state at infinity (Fig. 6). The matrix was imagined to obey J_2-deformation theory plasticity, and to follow the Ramberg-Osgood stress-strain curve

$$\varepsilon_m = \frac{\sigma}{E_m} \left[1 + \frac{3}{7} \left(\frac{\sigma}{\sigma_1} \right)^{n-1} \right] \qquad (30)$$

in uniaxial tension. Several earlier finite-element studies of this kind of problem have been made, notably in [15], but the presently reviewed calculations, executed on the basis of a trial-function variational approach, are the most complete to date. Up to 35 functions for the displacements in the matrix were used in the solution, and these were matched to an exact representation of the displacements in the elastic inclusion. Some sample results follow.

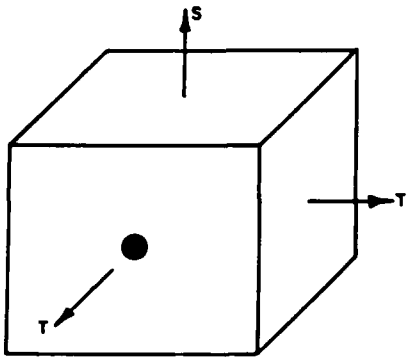

Fig. 6 Axisymmetric loading, isolated elastic inclusion

The stress of primary interest is the largest interface tension, σ_{max}, which usually occurs at the pole in the direction of S > T (Fig. 6). For the case of uniaxial tension (T=0), Fig. 7 shows how the stress-concentration factors

$$(SCF)_{pole} = \frac{\sigma_{pole}}{S} \quad , \quad (SCF)_{max} = \frac{\sigma_{max}}{S} \qquad (31)$$

vary with the level of applied stress, for the case n = 9, and three particle-matrix modulus ratios E_p/E_m = 1,2,4. (In each case, Poisson's ratio ν = 1/4 in both matrix and particle.) Depending on E_p/E_m, plasticity can either raise or lower the SCF with respect to its

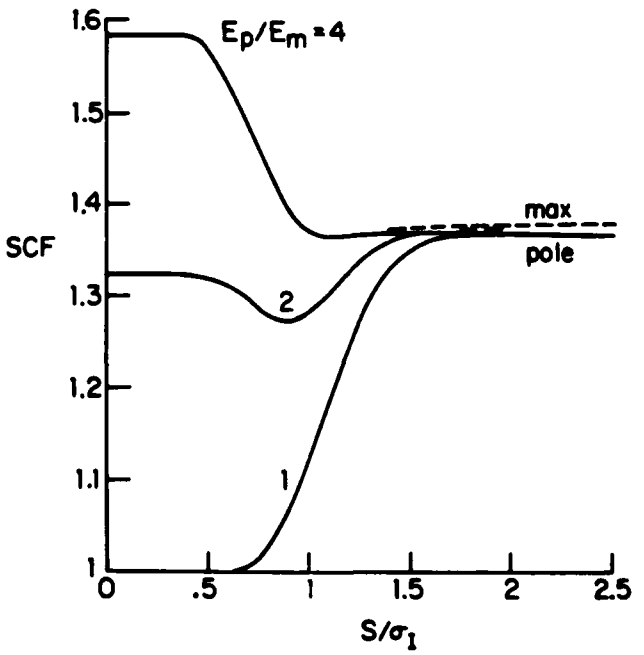

Fig. 7 Stress concentration factor, uniaxial loading, n = 9, $\nu_l = \nu_m$ = 1/4

elastic value. Note too, that for large applied loads, the SCF's for all E_p/E_m approach the same asymptotic value. This is because in the presence of much plastic deformation in the matrix an elastic inclusion becomes, effectively, rigid. For n = 9, the location of σ_{max} eventually moves about 13° off the pole at high loads; for still higher n, the shift can be as much as 18°.

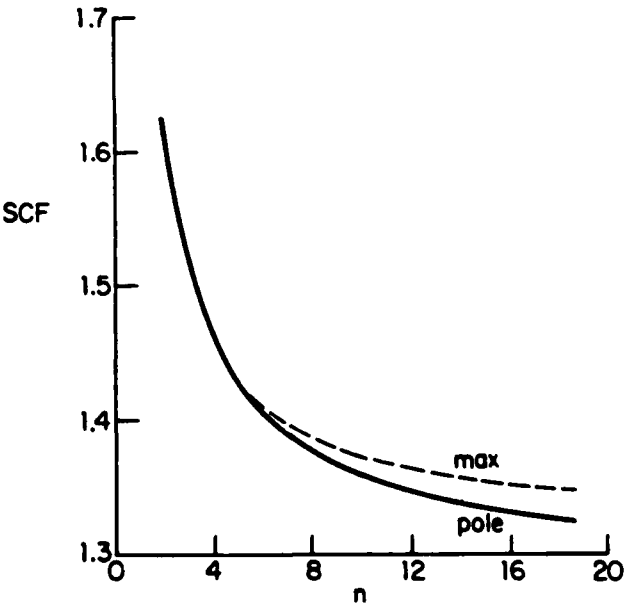

Fig. 8 Asymptotic stress concentration factors, $S/\sigma_l \to \infty$

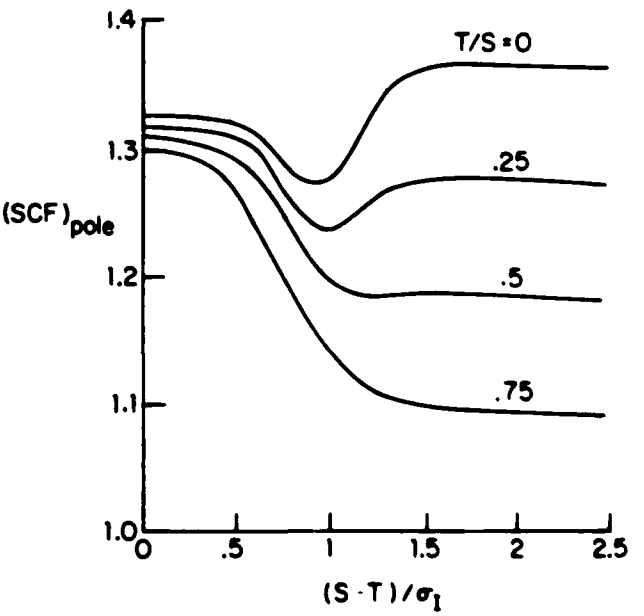

Fig. 9 Stress concentration factors, S > T ≥ 0, n = 9, E_p/E_m = 2, $\nu_p = \nu_m$ = 1/4

In Fig. 8, the asymptotic values of the SCF's are shown as a function of n. Note that even when the location of σ_{max} moves away from the pole, its value remains close to that of the pole stress. Finally, a sample set of results for S > T > 0 is shown in Fig. 9, for

the case $E_p/E_m = 2$, $\nu_p = \nu_m = 1/4$, and $n = 9$. Here $(SCF)_{pole}$ always drops initially as the effective stress (S–T) increases, but then approaches, not always monotonically, asymptotic values that decrease markedly with the amount of triaxiality present. This has some interesting implications. It is well known that triaxiality enhances void growth, once voids are nucleated. Accordingly, Fig. 9 indicates the possibilities of explosive void growth in the presence of triaxiality, since the delay of nucleation could set the void up for very rapid growth after it is produced by interfacial separation. On the other hand, it is interesting to note that in certain ranges of (S–T), where the curves of Fig. 9 have negative slopes, increasing T for a given S could *increase* the SCF.

LUNGS

This survey turns, finally, to a problem in biological micromechanics: how are the microscopic elastic constants of animal lungs related to the properties of their constituents? More precisely, we consider the spongy tissue in which the branching network of air passages in a lung culminates, and in which it is embedded. This tissue -- or *parenchyma* -- consists of a multitude of tiny polyhedral air sacs (*alveoli*), about 1/3 mm in diameter, with thin interfaces (like a mass of soap bubbles). When the lung is inflated to some internal pressure, the surrounding pleural membrane transmits tension to the parenchyma, to which it is attached. We will assume that the parenchyma is subjected to a state of hydrostatic tension, and ask: What are the elastic constants in the relation, presumed isotropic, between subsequent rates of stress and strain?

This problem was recently studied by Kimmel et al. [16] on the assumption that the alveoli could be idealized as regular dodecahedra, and, on the same basis, a still more recent analysis [17], based on a general variational principle of non-linear structural mechanics [18] was executed. The approach and results of [17] will be summarized here.

We contemplate an assemblage of polyhedra, each of which has half the thickness of the alveolar walls, focus attention on one of these hollow cells, and pretend that it is a regular dodecahedron (Fig. 10a). We will then assume that the relation between volume-averaged stress and strain in the isolated dodecahedron approximates

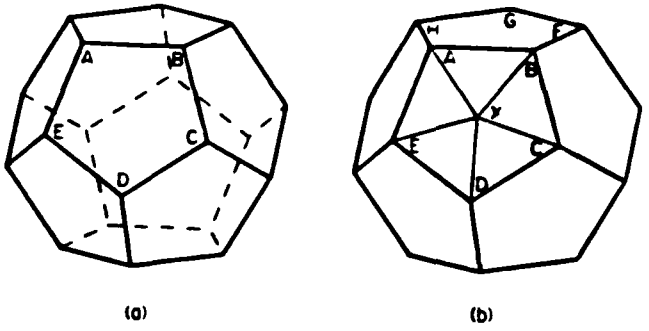

Fig. 10 (a) Regular dodecahedron, (b) subdivision of pentagonal faces

that for the parenchyma as a whole. However, to mimic the effect of mutual constraint among the alveoli, we will assume that when the dodecahedron deforms, the central displacement of each face is equal to the mean of its five corner displacements. Further, the displacements within each face will be assumed to vary linearly within each of the five triangles shown in Fig. 10b. Finally, we will throw all of the load-carrying capacity of the alveolar walls into idealized members along the edges of the dodecahedron. The constitutive relation connecting the tension T and length L of these members, and their rates-of-change, will be written, as in [16],

$$\dot{T}/T = B\dot{L}/L \tag{32}$$

where the non-dimensional modulus B could be a function of L.

Now apply a hydrostatic tension P to the faces of the dodecahedron. The incremental bulk modulus K defined by

$$K = \dot{P}/(\dot{V}/V) \tag{33}$$

was found in [16], as follows: By the principle of virtual work

$$P\dot{V} = 30\,T\dot{L} \tag{34}$$

but also

$$\dot{V}/V = 3\,\dot{L}/L \tag{35}$$

and consequently

$$PV = 10\,TL \tag{36}$$

so that, with the use of (32), the result

$$K/P = (B-2)/3 \tag{37}$$

follows. At B = 2, the structure becomes unstable.

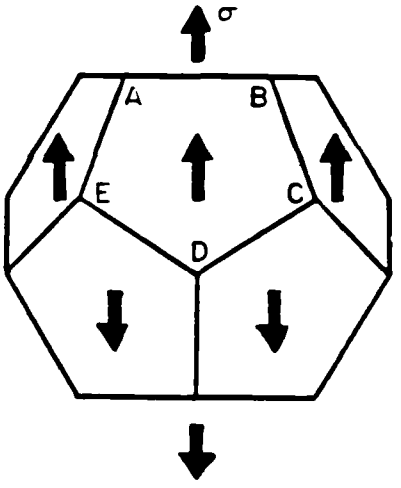

Fig. 11 Tensile loading σ

The determination of one more elastic constant is needed to characterize the material. With P held constant, the Young's modulus $E = \dot{\sigma}/\dot{\varepsilon}$ (Fig. 11) was calculated in [17] by the following approach. The principle of virtual work now says

$$\sum_{i=1}^{30} T_i \delta L_i = P\delta V + \delta\pi \tag{38}$$

where π is the potential of applied σ stresses. Because the structure is prestressed, non-linear terms in δL_i and δV must be retained in the implementation of (38). The algebra is messy, but ultimately, differentiation of (38) leads to linear equations relating corner velocities (there are just four essentially different ones) to $\dot{\sigma}$, and

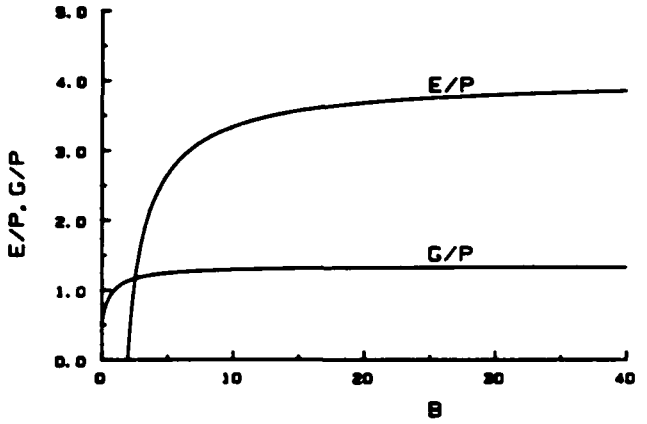

Fig. 12 Young's modulus E and shear modulus G, normalized by hydrostatic tension P

then, with a well-chosen definition for $\dot{e}$ in terms of the velocities, E can be computed. The result for E/P as a function of B is shown in Fig. 12, together with the curve for G/P (G = shear modulus) that follows from the standard connections among elastic constants of isotropic materials. The corresponding values for Poisson's ratio ν given by these connections are shown in Fig. 13.

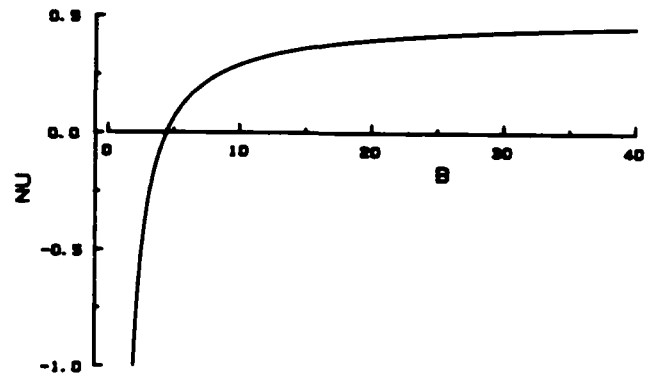

Fig. 13 Poisson's ratio ν

Note that for $B \to \infty$, the deformation becomes inextensional, yet the moduli E and G remain bounded, and proportional to P. (In fact, $E/P \to 5(1+\sqrt{5})/4 = 4.045$, and $\nu \to 1/2$ for $B \to \infty$). At the instability point B = 2, E vanishes, and ν = −1, but G remains finite.

It seems clear that the kinematic assumptions made for the deformation of the dodecahedron, together with its five-fold symmetry, ensure that it is indeed elastically isotropic. But to check this, Poisson's ratio was recomputed by means of a direct calculation of the transverse strain rates due to $\dot{\sigma}$, and the results were identical.

Some experimental informatior. on elastic moduli of animal lungs (dogs, pigs, horses), notably that due to Hajji et al. [19], has been interpreted in [16] to provide results that are roughly those of Fig. 12 for B ~ 5 – 30. (This range of B does correspond, more-or-less, to stressed biological materials in general.) A serious difficulty in the interpretation of experiments on inflated lungs is that the hydrostatic tension P in Eq. (37) and Fig. 12, is necessarily less than the inflation pressure P_I by an uncertain amount, namely the portion of P_I that is equilibrated by the pleural membrane and does not get transmitted back to the attached parenchyma. A rough estimate is $P/P_I \sim 3/4$, but the actual fraction is not independent of P_I, possibly dropping S as P_I goes up [19].

CONCLUDING REMARKS

The three sample problems of micromechanics reviewed here are quite different from each other, but there are many other flavors, represented by such topics as micro-buckling of fibers and surface layers, microcracking, interface tearing, micro-shear-banding, and the micromechanics of constrained phase transformations. Two points, in closing, lest the wrong impression be left by the present choice of topics: (a) a very important role has been played by sophisticated microscopic observations, and by microtesting techniques, that tell us what things really look like and what happens at microscopic scales; and (b) super-computing may assume an increasingly useful function in basic micromechanics research. Exploratory, massive, brute force calculations may provide results -- just like experiments do -- that inspire sensible mathematical modeling, and, at the other end of the game, numerical implementation of complex mathematical models will obviously be greatly facilitated.

ACKNOWLEDGEMENTS

This work was supported in part by the Office of Naval Research under Contract N00014-84-K-0510, and by the Division of Applied Sciences, Harvard University.

REFERENCES

1. Budiansky, B., "Micromechanics", Computers and Structures, Vol. 16, No. 1-4, 1983, pp. 3-12.

2. Budiansky, B., Hutchinson, J. W. and Lambropoulos, J. C., "Continuum Theory of Dilatant Transformation Toughening in Ceramics", Int. J. Solids Structures, Vol. 19, No. 4, 1983, pp. 337-355.

3. McMeeking, R. M., and Evans, A. G., "Mechanics of Transformation Toughening in Brittle Materials", J. Am. Ceram. Soc., Vol. 65, 1982, pp. 242-246.

4. Lambropoulos, J. C., "Shear, Shape and Orientation Effects in Transformation Toughening", to be published in Int. J. Solids Structures.

5. Evans, A. G., and Cannon, R. M., "Toughening of Brittle Solids by Martensitic Transformations", Acta. Met., Vol. 34, No. 5, 1986, pp. 761-800.

6. Budiansky, B., Hutchinson, J. W., and Evans, A. G., "Matrix Fracture in Fiber-Reinforced Ceramics", J. Mech. Phys. Solids, Vol. 34, No. 2, 1986, pp. 167-189.

7. Krstic, V. D., Nicholson, P. S. and Hoagland, R. G., "Toughening of Glasses by Metallic Particles", J. Am. Ceram. Soc., Vol. 64, No. 9, 1981, pp. 499-504.

8. Krstic, V. D., "On the Fracture of Brittle-Matrix/Ductile-Particle Composites", Phil. Mag. A, Vol. 48, No. 5, 1983, pp. 695-708.

9. Sigl, L. S., "Das Zähigkeitsrerhalten von Wc-Co Legierungen", Dissertation, Montanuniversität Leoben, Stuggart, Mai 1985.

10. Budiansky, B., Amazigo, J. C., and Evans, A. G., research in progress.

11. Evans, A. G., personal communication.

12. Evans, A. G., and McMeeking, R. M., "On the Toughness of Ceramics by Strong Reinforcements", research in progress.

13. Marshall, D. B., and Evans, A. G., "The Tensile Strength of Uniaxially Reinforced Ceramic Fiber Composites", in *Fracture Mechanics of Ceramics*, Ed. R. C. Bradt, A. G. Evans, B. P. H. Hasselman, and F. F. Lange, Vol. 7, Plenum, 1986, in press.

14. Wilner, B., "Stress Analysis of Particles in Metals", Ph.D. Thesis, Harvard University, 1986.

15. Thomson, R. D., and Hancock, J. W., "Local Stress and Strain Fields Near a Spherical Elastic Inclusion in a Plastically Deforming Matrix", Int. J. Frac., Vol. 24, 1984, pp. 209-228.

16. Kimmel, E., Kamm, R. D., and Shapiro, A. H., "A Cellular Model of Lung Elasticity", 1986, to be published.

17. Budiansky, B., and Kimmel, E., "Elastic Moduli of Lungs", Rept. MECH-78, Division of Applied Sciences, Harvard University, May 1986.

18. Budiansky, B., "Remarks on Theories of Solid and Structural Mechanics", *Problems of Hydrodynamics and Continuum Mechanics*, L. I. Sedov Birthday, SIAM, 1969, pp. 77-83.

19. Hajji, M. A., Wilson, T. A., and Lai-Fook, S. J., "Improved Measurements of Shear Modulus and Pleural Membrane Tension of the Lung", J. Appl. Physiology: Respiratory and Environmental Exercise Physiology, Vol. 47, 1979, pp. 175-181.

END

DTIC

9-86